REVIEW

Check for updates

Synthesis and applications of conjugated main-chain charged polyelectrolytes

Hai-Yan Huang,[a,b] Dongyang Fan,*[b] Dong Wang, [ID] [b] Ting Han [ID] *[b] and Ben Zhong Tang [ID] *[c]

Conjugated main-chain charged polyelectrolytes (CMCPs) represent an important class of functional polymeric materials exhibiting distinctive structures and properties. By merging the advantages of conjugated polymers with the charge modulation capabilities of electrolytes, CMCPs have found wide applications in different fields and have garnered considerable interest across multiple disciplines such as chemistry, chemical engineering, materials science, and biomedicine. In this review, we emphasize the progress in the synthetic strategies of different types of CMCPs, including pyridinium-containing CMCPs, imidazolium-containing CMCPs, and other related structures. Furthermore, the applications of CMCPs in antimicrobial reagents, fluorescence sensing, fluorescence imaging, cancer cell killing, and fiber preparation are also introduced. To provide insights into the development of novel CMCPs with advanced functionalities, the current challenges and future prospects in this field are addressed at the end of this review.

[a] *College of Chemistry and Environmental Engineering, Shenzhen University, Shenzhen, Guangdong 518060, China*
[b] *Center for AIE Research, Guangdong Provincial Key Laboratory of New Energy Materials Service Safety, College of Materials Science and Engineering, Shenzhen University, Shenzhen, Guangdong 518060, China. E-mail: dongyang.fan@szu.edu.cn, hanting@szu.edu.cn*
[c] *School of Science and Engineering, Shenzhen Institute of Aggregate Science and Technology, The Chinese University of Hong Kong, Shenzhen, (CUHK-Shenzhen), Guangdong 518172, China. E-mail: tangbenz@cuhk.edu.cn*

1. Introduction

Polyelectrolytes are a class of important functional polymeric materials with ionizable groups, exhibiting the advantages of both functional polymers and electrolytes. Natural polyelectrolytes, such as DNA/RNA, polysaccharides, proteins, and peptides, play important roles in life activities.[1,2] On the other hand, synthetic polyelectrolytes, which are prepared by artificial approaches with designable structures and diversified functionalities, have been widely applied in the fields of chemistry, chemical engineering, materials science, biological and biomedical sciences, *etc*.[3–8] According to the location of

Hai-Yan Huang is currently pursuing her PhD degree under the supervision of Prof. Ting Han at Shenzhen University. Her research interests mainly focus on the synthesis and applications of functional fluorescent polyelectrolytes based on polymerization of acetylenic monomers.

Hai-Yan Huang

Dongyang Fan received his PhD degree from Shanghai Jiao Tong University in 2019 under the supervision of Prof. Wanbin Zhang. Later, he worked as a post-doctoral fellow at Nanyang Technological University and Shenzhen University. He is currently an associate researcher at Shenzhen University. His research interests focus on the design, synthesis and applications of fluorescent heterocyclic polymers based on polymerization of triple-bond monomers.

Dongyang Fan

charges, polyelectrolytes can be categorized into side-chain charged polyelectrolytes (SCPs, where the charged units are attached to the side chains) and main-chain charged polyelectrolytes (MCPs, where the charges are located on the polymer backbone). Among SCPs, lots of backbone structures, such as poly(thiophene)s, poly(fluorene)s, poly(*p*-phenylene)s, poly(*p*-phenylenevinylene)s, poly(*p*-phenylene ethynylene)s, poly(diketopyrrolopyrrole)s, *etc*. have been reported.[9] The common charged units of SCPs include groups such as quaternary ammonium, phosphonium, carboxyl, sulfonic, phosphate, pyridinium, imidazolium, *etc*., which are generally located at the end of the side chains.[7,10–17] Such a structural feature restricts the direct influence of ionizable groups on the electronic properties of the polyelectrolyte backbones. In contrast, the charges of MCPs are directly located within the polymeric chromophores, which provide great convenience for the regulation of electronic structures and physicochemical properties. Taking advantage of the inherently strong electron-donating/ withdrawing ability of the ionized motifs in the polymer main chain, the photophysical properties and phototherapeutic effects of MCPs can be modulated easily.[2,18] Furthermore, compared to SCPs, MCPs are expected to exhibit significantly different intra/inter-chain interactions, such as anion–π^+ interactions, which can further affect their photophysical properties, while the coexistence of polar and non-polar groups in the main chain may contribute to their solution processability.[2,8,19,20] In addition, MCPs usually have higher stability and higher charge density. By attaching different types of ionic functional groups to the backbones of MCPs, the MCPs could be endowed with different features. Thus, MCPs have promising potential for multifunctional applications.[3,4]

Specifically reported backbones of MCPs include non-conjugated and conjugated types that contain different ionic motifs such as ammonium, phosphine, sulfonium, selenium, piperidinium, imidazolium, and pyridinium.[21–27] Compared to non-conjugated MCPs, conjugated MCPs (CMCPs) exhibit excellent optoelectronic properties, high mechanical strength and thermal stability, and the molecular wire effect, which are well-inherited from the intrinsic advantages of conjugated polymers. The molecular wire effect could facilitate the communication of electrical signals or electrons along the conjugated polymer backbones, thus showing enhanced sensitivity as fluorescence sensors. These properties allow CMCPs to show great potential in the fields of high-performance electronic devices, optoelectronic materials, fluorescent chemo-/ biosensors, biological imaging, and biomedicine.[8,9,28–31] Current research studies on polyelectrolytes mainly focus on SCPs,[10–17] while relevant studies of MCPs, especially CMCPs, remain insufficient, primarily due to the challenges in their synthesis. Based on previous studies, conjugated polyelectrolytes can be achieved through direct polymerization of monomers containing ionic functional groups. Related strategies include Wessling polymerization, oxidative polymerization, the Gilch synthesis method, and Suzuki, Sonogashira, Heck and Stille polycouplings.[31–35] Direct polymerization strategies can yield target products efficiently in a one-step manner. However, these methods often require pre-functionalized ionic monomers, resulting in a narrow range of monomers, and the corresponding polymerization often suffers from harsh reaction conditions and poor atomic economy. The other kind of strategy is indirect synthesis, in which neutral conjugated polymer backbones are prepared first, followed by the introduction of charged groups on the backbones by post-modifications.[36–38] These strategies feature the advantages of high polymerization flexibility, wider monomer selections, and controllable charge types. However, post-modifications cannot always be accomplished completely and are often accompanied by difficult-to-remove by-products, which may affect the performance and application of polyelectrolytes. Recently, another emerging strategy, named the C–H activation/annula-

Ting Han

Ting Han received her BS degree from the Beijing Institute of Technology in 2014, and obtained her PhD degree from the Hong Kong University of Science and Technology (HKUST) in 2018 under the supervision of Prof. Ben Zhong Tang. After her post-doctoral studies in Prof. Ben Zhong Tang's group at HKUST, she joined Shenzhen University in 2019. She is now an associate professor and a specially appointed researcher at Shenzhen University. Her research interests include the development of new alkyne-based polymerization reactions and the design, synthesis, and applications of functional luminescent polymers.

Ben Zhong Tang

Ben Zhong Tang received his BS and PhD degrees from South China University of Technology and Kyoto University in 1982 and 1988, respectively. He conducted his postdoctoral work at the University of Toronto from 1989 to 1994. He joined HKUST in 1994 and was promoted to Chair Professor in 2008. He was elected to the Chinese Academy of Sciences in 2009. In 2021, he joined CUHK-Shenzhen as the Dean of the School of Science and Engineering. His research interests include the exploration of new advanced materials, new luminescent processes, and new polymerization reactions.

tion polymerization (CAAP) strategy, has been applied to the synthesis of CMCPs.[29,39] Such polymerizations are highly efficient and environmentally friendly, with broad monomer selectivity and high atom economy, which allow the *in situ* construction of CMCPs with complex and diverse structures and promote the emergence of more multifunctional polymeric materials.

Despite the emergence of numerous systematic review studies in the field of conjugated polyelectrolytes,[32,40–42] a comprehensive review of CMCPs is still lacking. Considering the significance of CMCP materials, this review aims to fill this gap by summarizing the progress in the synthetic methods and application of CMCPs. First, the synthetic strategies for CMCPs containing pyridinium, imidazolium, and other backbones, such as those with phosphonium and cinnolinium salts, are presented. The involved synthetic strategies include ring-transmutation polymerization, nucleophilic substitution, aldol-type polycondensation, CAAP, *etc*. Furthermore, based on the inherent excellent photophysical properties, high electrical conductivity, good film-forming properties, and biological activities of CMCPs, their applications in antimicrobial reagents, fluorescence sensing, fluorescence imaging, cancer cell killing, and fiber formation are also introduced. Finally, a brief summary and some perspectives on the future development directions of CMCPs are discussed.

2. Synthesis of CMCPs

CMCPs have received widespread attention in recent years due to their unique structures and attractive properties. Synthesis methods for CMCPs range from traditional polymerization reactions to emerging new synthetic strategies. From the perspective of structures, CMCPs mainly include pyridinium-containing backbones and imidazolium-containing backbones. In this section, we will mainly introduce the current progress in the synthesis of pyridinium-containing and imidazolium-containing CMCPs, although the synthesis strategies of phosphonium- and cinnamonium-type polyelectrolytes will also be briefly discussed.

2.1 Synthesis of pyridinium-containing CMCPs

2.1.1 Ring-transmutation polymerizations. The pyridinium ring is one of the most commonly reported ionized structural units of CMCPs. An effective and widely used method for the construction of pyridinium-containing CMCPs is ring-transmutation polymerization, which refers to the polymerization of oxygenated pyrylium salts with aromatic diamines to form nitrogen-containing polypyridinium salts. In this method, pyrylium compounds are commonly employed as monomers to react with amines, and pyridinium rings are formed *via* the replacement of the oxygen atoms in pyrylium by nitrogen atoms *via* ring-transmutation reactions. The synthetic routes of pyrylium monomers are shown in Fig. 1A as an example. First, terephthalaldehyde is reacted with acetophenone to afford the tetraketone (compound **1**). Subsequently, compound **1** undergoes cyclodehydration in the presence of triphenylmethyl tosylate to generate the pyrylium monomer **2**. By polymerizing the pyrylium monomer **2** with diamine monomers through a ring-transmutation polymerization reaction, pyridinium-containing polymers **P1** can be produced efficiently. Further reactions with different salts *via* the metathesis mechanism can give polymers **P2** with different anions (Fig. 1B and C).

For example, Sun *et al.* reported the preparation of conjugated polypyridinium salts by ring-transmutation polymerization of a bis(pyrylium salt) (**2a**) and 3,6-diamino-*N*-butylcar-
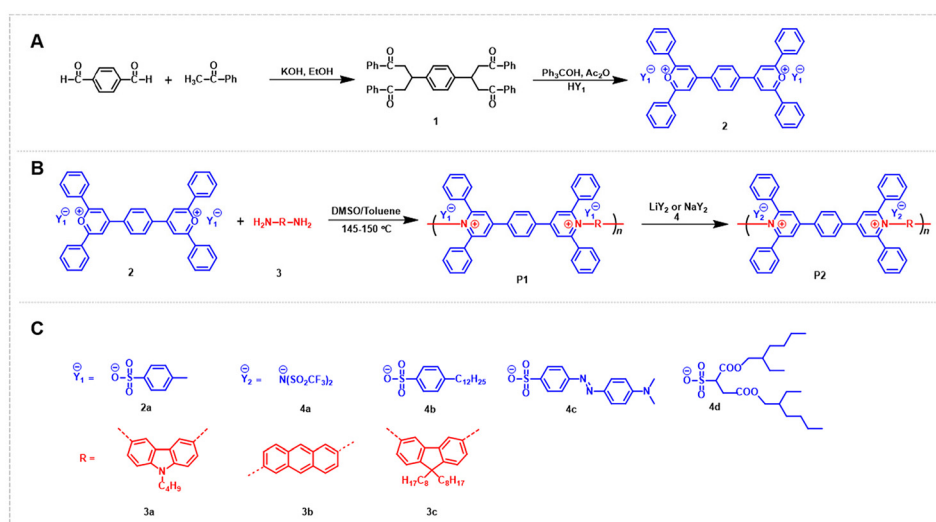

Fig. 1 Synthetic routes of pyridinium-containing CMCPs *via* ring-transmutation polymerizations. (A) Synthesis routes of pyrylium salts. (B) Polymerizations between pyrylium salts and amines to form pyridinium-containing CMCPs. (C) Chemical structures of different anions (**2a** and **4a–d**) and amine monomers (**3a–c**) used for the preparation of CMCPs. Adapted with permission from ref. 20 (Copyright 2013 the Royal Society of Chemistry), ref. 43 (Copyright 2006 Elsevier), and ref. 44 (Copyright 2021 MDPI).

bazole (**3a**).[20] The polymerization was carried out in DMSO, followed by the addition of toluene, and the resulting water could be removed as a toluene/water azeotrope. The yield was more than 85% with a number-average molecular weight (M_n) of 13 800 g mol^{-1}. Notably, the polymer exhibited typical aggregation-induced emission (AIE) properties. Therefore, the fluorescence of the polymer largely increased upon aggregation by electrostatic interactions with DNA, allowing for its application in sensitive DNA detection. Besides, Bhowmik *et al.* developed the ring-transmutation polymerization of a phenylated bis(pyrylium tosylate) salt (**2a**) and 2,6-diaminoanthracene (**3b**), producing an anthracene-containing polypyridinium after reacting for 24 h at 145–150 °C.[43] By using lithium triflimide (**4a**), the counterions of CMCPs could be converted from tosylate to triflimide. In this study, the emission wavelengths of two obtained polymers were lower than 400 nm both in solution and in the solid state, exhibiting UV-light fluorescence. Furthermore, these polymeric products showed lyotropic liquid crystal properties and good film formation abilities, which endowed them with potential in optoelectronic applications. In 2021, this group further developed a series of poly (pyridinium salt)-fluorene CMCPs (**4a–d**) containing different anions by this method.[44] The M_n values of these CMCPs ranged from 96 500 to 107 800 g mol^{-1}. Due to the introduction of bulky counterions, the glass transition temperature (T_g) values decreased for some of the polyelectrolytes, and the thermal stability ranged from 305 to 423 °C. In addition,

regardless of the counterion structures, all polyelectrolytes could form aggregates in DMSO, CH$_3$CN, and CH$_3$OH with the addition of water and the emission peaks of these aggregates gradually blue shifted. The above-mentioned approach for preparing pyridinium-containing CMCPs by ring-transmutation polymerization is well established and widely employed. By altering the conjugated backbone and anion structures, the properties of CMCPs can be easily tuned to meet the demands of different practical applications.

2.1.2 Nucleophilic substitution polymerizations and aldol-type polycondensations.

In addition to ring-transmutation polymerizations, nucleophilic substitution polymerizations and aldol-type polycondensations can also be used to synthesize CMCPs. As depicted in Fig. 2A, theoretically speaking, CMCPs containing pyridinium structures can be prepared by nucleophilic substitution polymerizations using 4,4′-bipyridine or its derivatives with dibromides as monomers. However, this method has been mainly employed to synthesize non-conjugated MCPs. In the reported studies, R$_1$ could be viologen derivatives, alkyl chains, azo structures, *etc.*, while alkyl chains containing different numbers of carbon atoms are often used as R$_2$ moieties.[45–47] In contrast, post-modification reactions based on nucleophilic substitutions have been widely utilized to prepare pyridinium-containing CMCPs. For instance, in 2009, Swager *et al.* synthesized a type of water-soluble n-type polymer bearing pyridinium-phenylene units.[48] As depicted in Fig. 2B, monomer **6** was first synthesized *via* the preparation
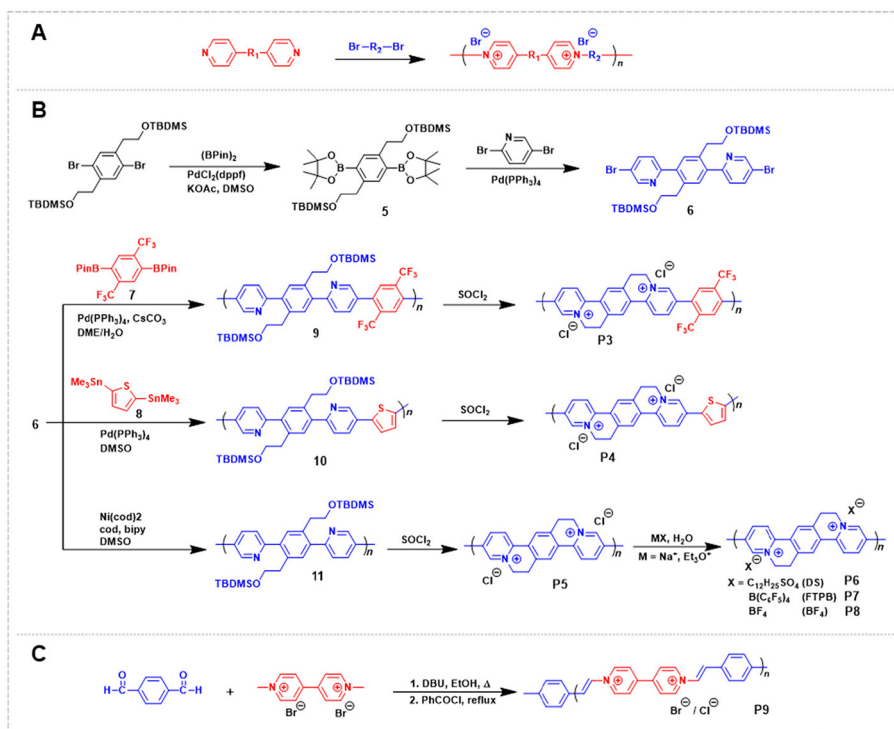
Fig. 2 (A) The common method used for the synthesis of non-conjugated MCPs. (B and C) Synthesis of pyridium-containing CMCPs *via* (B) nucleophilic substitution reactions and (C) aldol-type polycondensations. Adapted with permission from (B) ref. 48 (Copyright 2009 American Chemical Society), ref. 49 (Copyright 2014 Wiley-VCH GmbH), and (C) ref. 50 (Copyright 1989 Wiley-VCH), respectively.

of borate ester **5** *via* a boronation reaction and a sequential Suzuki coupling reaction. Next, pyridyl precursor-polymers (**9**, **10**, and **11**) were prepared by Suzuki, Stille and Yamamoto polycoupling reactions, respectively, in order to obtain polymers with different structures, and the yields of these coupling polymerizations can reach up to 95%. In the presence of SOCl₂, intramolecular nucleophilic substitution reactions were then used to form pyridinium rings in the targeted polyelectrolytes (**P3**, **P4**, and **P5**). All the obtained CMCPs exhibited high electron affinities, reversible redox behavior, high electrical conductivity, and good electron mobilities, indicating a promising class of advanced functional polymer materials. In 2014, Swager *et al.* further developed a series of CMCPs using the anion exchange reactions of **P5**.[49] The presence of different anions endowed the polymers (**P6**, **P7**, and **P8**) with different solubility, optical properties, and sensing responsiveness. Taking the detection of volatile amines as an example, **P5** was most responsive to pyridine, while **P7** and **P8** showed the best sensing abilities to simple alkyl amines and aniline, respectively. These polymers can detect analytes at low ppm concentrations, which are close to or below permissible exposure limit values.

Aldol-type polycondensation is another commonly used strategy for the synthesis of pyridinium-containing CMCPs. This method usually employs bisaldehydes and bipyridine derivatives as monomers, which undergo polycondensations under alkaline conditions to produce target products. As shown in Fig. 2C, Merz *et al.* synthesized a conductive bipyridium polymer *via* this method.[50] The reaction was carried out with methylbipyridine and 1,4-benzenedicarboxaldehyde as monomers in the presence of the organic base 1,8-diazabicyclo [5.4.0]undec-7-ene (DBU) and the dehydrating agent benzoyl chloride to obtain the polyelectrolyte **P9**, which has a conductivity of 1×10^{-3} S cm^{-1} and electroactivity in the range from −0.1 to −0.6 V *versus* Ag/AgCl. More importantly, **P9** showed good stability in water and many organic solvents. When exposed to iodine vapors, the conductivity of **P9** can be further increased 2–3-fold.

2.1.3 Alkyne-based polymerizations. The aforementioned sections introduced the traditional methods for the synthesis of pyridinium-containing CMCPs. In recent years, with the vigorous development of organic chemistry, a number of novel polymerization strategies based on small-molecule organic reactions have been explored by polymer chemists and these methods are capable of synthesizing novel CMCPs conveniently and even more efficiently. Among them, alkyne-based polymerizations not only can endow polymers with excellent optoelectronic properties, mechanical strength and diverse structures, but also have highly controllable functionalization potential, which are favorable for the development of CMCPs with attractive performance and advanced applications.

For instance, Qin *et al.* recently developed a novel spontaneous amino-yne click polymerization reaction with diamine (**13**) and pyridinium-activated diyne (**12**) as monomers to prepare a series of pyridinium-containing CMCPs **P10** in yields
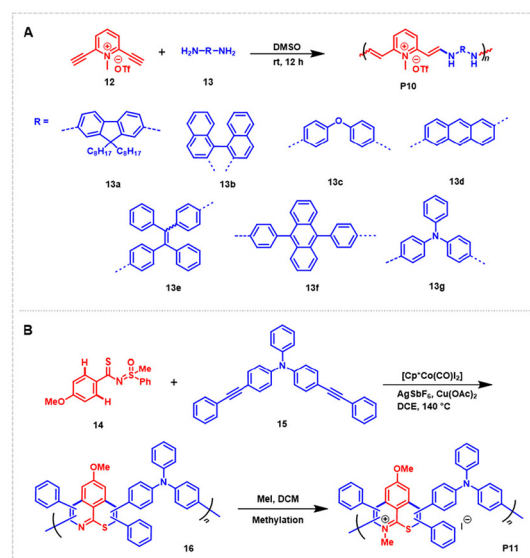
Fig. 3 (A and B) Alkyne-based two-component polymerization methods. Reproduced with permission from (A) ref. 51 (Copyright 2024 ChemRxiv) and (B) ref. 52 (Copyright 2024 American Chemical Society), respectively.

of up to 98% with an M_w of up to 22 200 g mol^{-1} (Fig. 3A).[51] The resulting polyelectrolytes all exhibited excellent thermal stability and were made to have good aggregate-state luminescence by introducing AIEgens into the polyelectrolyte backbone. In addition to the click polymerizations, alkyne-based C–H activation/annulation polymerizations (CAAPs) have also been used to synthesize CMCPs. Very recently, Fan *et al.* reported a cobalt(III)-catalyzed CAAP method using aryl thioamides (**14**) and internal alkynes (**15**) as starting materials for the preparation of N, S-doped fused heterocyclic polymers (**16**) (Fig. 3B).[52] The corresponding polyelectrolyte (**P11**) was then obtained *via* post-methylation of the polymer. Interestingly, the refractive index values of **P11** at 632.8 nm and 1550 nm were up to 1.8464 and 1.7869, respectively, exhibiting low chromatic dispersions. This polymerization strategy was facile, straightforward, and efficient, which enhanced the possibility of constructing CMCPs with various structures and functionalities.

Apart from two-component alkyne-based polymerization methods, Tang *et al.* successfully developed several multicomponent CAAP reactions to synthesize pyridinium-containing CMCPs. For example, a rhodium-catalyzed multicomponent CAAP strategy using readily accessible monomers has been developed (Fig. 4A).[2] This method can efficiently synthesize a series of azonia-containing polyelectrolytes in a one-pot manner (up to 99% yield and 28 700 Da molecular weight). Owing to the presence of electron-deficient azonia-containing fused rings in the main chains, the emission wavelength of **P12** can be tuned by changing the electron donors. Meanwhile, the obtained CMCP films displayed efficient solid-state luminescence with good photosensitivity and high refractive indices. These properties allowed the polymers to be
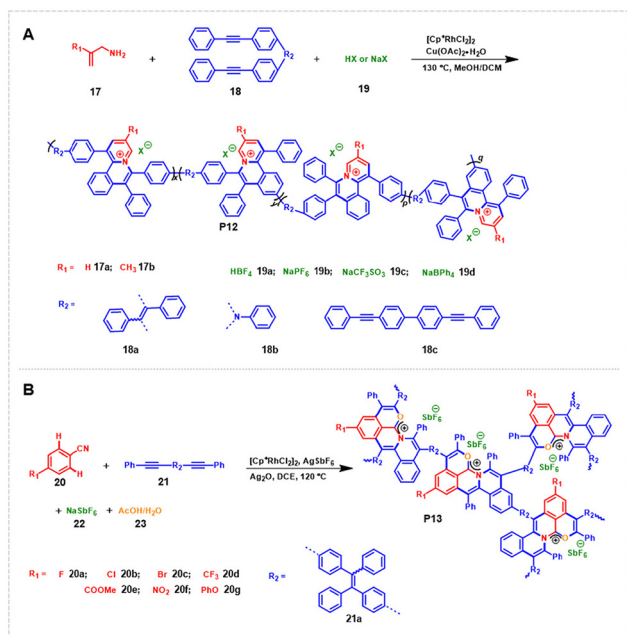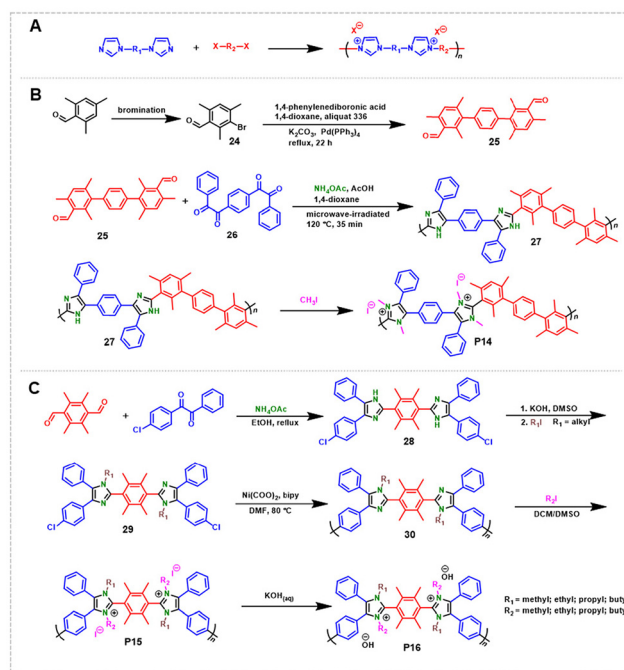
Fig. 4 (A and B) Alkyne-based multicomponent polymerization methods. Reproduced with permission from (A) ref. 2 (Copyright 2019 American Chemical Society) and (B) ref. 18 (Copyright 2021 Wiley-VCH GmbH), respectively.

Fig. 5 (A) The synthetic method of non-conjugated MCPs with imidazolium-salts. (B and C) The synthetic routes of imidazolium-containing CMCPs *via* the post-modification reaction. Reproduced with permission from (B) ref. 55 (Copyright 2017 American Chemical Society) and (C) ref. 56 (Copyright 2019 Springer Nature), respectively.

potentially applied in fluorescence photopatterning and advanced optical materials. In 2021, this group further synthesized a series of heteroaromatic hyperbranched polyelectrolytes in a one-pot manner by multicomponent CAAP in up to 97% yield (Fig. 4B).[18] Compared to traditional approaches, the method required neither expensive monomers nor strict conditions, and enjoyed the applicability of a wide range of monomers. Similarly, the D–A structures in polymers allowed for tunable luminescence properties.

Overall, alkyne-based polymerization methods have created new development room to synthesize pyridium-containing CMCPs. It can be foreseen that this type of synthetic method and the obtained fused heterocyclic polyelectrolytes will provide more opportunities for the development of advanced functional polymer materials through further exploration of the structural design, synthesis and structure–property relationship.
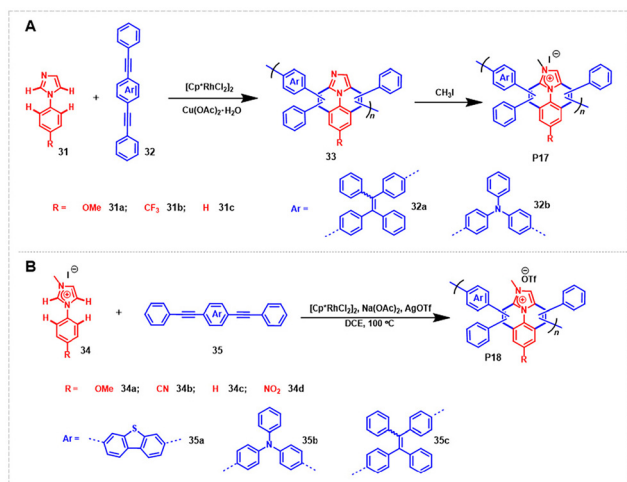
2.2 Synthesis of imidazolium-containing CMCPs

In addition to pyridinium salts, imidazolium has been reported as being another commonly used ionization motif for the design of CMCPs. Theoretically speaking, diverse imidazolium-containing CMCPs could be conveniently synthesized by a nucleophilic substitution polymerization strategy of reacting bisimidazole monomers with aryl dihalides (Fig. 5A).[53,54] Regretably, to the best of our knowledge, this strategy has only been applied for the preparation of imidazolium-containing non-conjugated MCPs using aliphatic bisimidazole monomers and aryl dihalides.

One of the most popular strategies for constructing imidazolium-containing CMCPs is the post-modification method. For example, Holdcroft *et al.* synthesized poly(arylene-imidazole) (**27**) by a microwave-irradiated polycondensation reaction using dialdehyde, bis(dibenzoyl), and ammonium acetate as monomers. The methylation reaction of **27** eventually affords the imidazolium-containing polyelectrolyte **P14** with an M_w of 67 000 g mol^{-1} in a yield of 95% (Fig. 5B).[55] The resulting polyelectrolyte showed excellent stability with a half-life of more than 5000 h at 100 °C in 10 M KOH aqueous solution. The films of the polyelectrolyte were tough, pliable and transparent. The tensile strength was 43.5 ± 1.4 MPa and elongation at break was 44.3 ± 9.6%. Besides, this group prepared imidazole-containing polymers **30** by Yamamoto homopolycoupling using synthesized dichloroimidazole compounds as monomers. Then, the imidazole structure of the polymer was alkylated to obtain imidazolium CMCPs (**P15**) (Fig. 5C).[56] The obtained products showed good solubility. These bisimidazolium polymers and membranes exhibited balanced alkaline stability and high ion-exchange capacity, resulting in exceptional chemical stability and hydroxide conductivity with minimal water content.

The CAAP strategy can be employed for the synthesis of imidazolium-containing CMCPs as well. Recently, Wang *et al.* reported an efficient rhodium-catalyzed cascade CAAP strategy for the synthesis of polymers with multiple ring-fused aza-heteroaromatic structures from aryl imidazoles (**31**) and internal

Fig. 6 (A and B) Synthesis of imidazolium-containing CMCPs based on the C−H activation/annulation polymerization strategy. Reproduced with permission from ref. 29 (Copyright 2022 American Chemical Society) and ref. 8 (Copyright 2023 American Chemical Society), respectively.

diynes (**32**) (Fig. 6A).[29] Polybenzoimidazoles (**33**) containing rigid conjugated spacers of tetraphenylene (TPE) or triphenylamine (TPA) were prepared in up to 96% yield within 2 h. These conjugated polymers showed good thermal and morphological stability, retaining more than 70% of the char residue at 800 °C, with glass transition temperature (T_g) values as high as 315 °C. Imidazolium-containing CMCPs (**P17**) were further afforded *via* the simple *N*-methylation reaction of **33** in nearly quantitative yields with red-shifted fluorescence emission. Due to the highly separated charge distribution in the CMCPs, the energy gap between singlet and triplet states was apparently reduced, which promoted the intersystem crossing process, giving these CMCPs strong ROS-generating ability and excellent performance in cancer cell killing. Following this work, this group further reported an N-heterocyclic carbene-directed cascade CAAP strategy for the direct preparation of fluorescent cationic CMCPs in up to 97.2% yield (Fig. 6B).[8] This rhodium-catalyzed polymerization proceeded smoothly under mild conditions with readily available monomers (**34** and **35**). The generated CMCPs (**P18**) have good solubility in commonly used organic solvents. By introducing different substituents around the cationic ring-fused core, the donor–acceptor effect in the polymers could be effectively regulated, which further enhances the tuning flexibility of fluorescence properties of these CMCPs.

The abovementioned examples indicated that the CAAP strategy is an attractive method for the development of multi-substituted imidazolium-containing CMCPs with diversified structures in a simple, straightforward, atom-economical, and efficient manner. Further development of novel CAAP reactions will provide more convenience to prepare novel imidazolium-containing CMCPs with fascinating functionalities. Meanwhile, the CAAP strategy also faces several challenges.

For instance, the CMCP products obtained through this method are often composed of multiple isomeric repeating units. The poor structural regularity of such CMCPs is favorable for solubility and processability but may limit their application performance in certain areas like electrical devices.

2.3 Synthesis of other CMCPs

In addition to the aforementioned pyridinium and imidazolium salts, which are the most commonly reported types of charged motifs for CMCPs, other CMCPs with other types of charged units will be briefly introduced in this section.

For example, Anderson *et al.* reported a strategy for the synthesis of phosphonium-containing CMCPs (Fig. 7).[31] First, compound **36** was prepared by a Knoevenagel condensation reaction between bromothiophene aldehyde and 1,4-diacetyl-2,5-diketopiperazine. Subsequently, compound **36** was prepared in the presence of Tf₂O to give compound **37**. Finally, the substitution reaction of compound **37** with triphenylphosphonium afforded phosphonium-containing monomer **38** (Fig. 7A). The Stille polycoupling of monomer **38** with different tin-functionalized thiophene monomers gave phosphonium-containing CMCPs with different main chains (**P19**, **P20**) (Fig. 7B). Optical, electrochemical and theoretical studies revealed that these ionic substituents endowed the polyelectrolytes with low LUMO energy levels and small and highly tunable band gaps. Both polyelectrolytes exhibited NIR absorbance and **P19** exhibited excellent photothermal properties under 808 nm laser irradiation, showing great potential in antimicrobial photothermal therapy (PTT). Furthermore, Zhang *et al.* developed a Rh(III)-catalyzed polymerization process using internal alkynes and azo compounds to obtain cinnolinium-containing CMCPs.[57] The synthesized polyelectrolyte had an M_w of 25 000 g mol⁻¹ and good thermal stability. Benefiting from the unique luminescence properties and the positive-charged cores, the polyelectrolyte was successfully applied in bacterial imaging and killing.
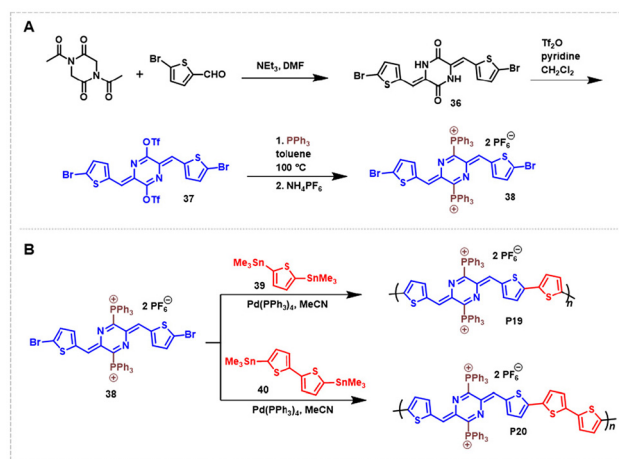
Fig. 7 (A and B) The synthetic route of CMCPs with a phosphonium-salt structure. Adapted with permission from ref. 31. Copyright 2019 Wiley-VCH GmbH.

As a short summary, with the advancement of different synthetic strategies, a number of CMCPs have been developed in the past years. However, the structural diversity of CMCPs still needs to be further enriched.

3. Applications of CMCPs

The unique structures of CMCPs endow them with a variety of properties, including good photoluminescence, liquid crystallinity, thermal stability, high electrical conductivity, and biological activity.[9] These properties expand their potential applications in solar cells, anion-exchange membranes, and devices for cell imaging, sensing, fluorescence photo-patterns, and so on. This section focuses on representative examples of the applications of CMCPs.

3.1 Antibacterial applications

Generally, the bacterial membrane surface is negatively charged owing to the presence of carboxylate, sulfate, phosphate groups, *etc.*[58] Positively charged CMCPs tend to bind to bacterial membranes through electrostatic interactions and potentially induce dark toxicity to bacteria. Furthermore, certain CMCPs demonstrate strong reactive oxygen species (ROS) generation capabilities, enabling their applications in photodynamic bacterial killing.

In recent years, Tang's group reported the synthesis of a series of azonia-containing polyelectrolytes in a one-pot manner.[2] The resulting polyelectrolytes exhibited typical AIE characteristics, photostability and rapid bacterial staining capacities. More importantly, they possessed excellent ROS

generation ability to kill methicillin-resistant *Staphylococcus aureus* (MRSA), showing good bactericidal effects both *in vitro* and *in vivo*. Susequently, this group further reported a rhodium(III)-catalyzed CAAP strategy for constructing nitrogen-containing fused hyperbranched polyelectrolytes.[18] As depicted in Fig. 8A and B, the CMCP **P21** containing a tetraphenylethylene (TPE) unit exhibited aggregation-enhanced emission (AEE) with its emission intensity significantly increasing upon the addition of a poor solvent. Using ROS indicators, **P21** demonstrated strong $^1O_2$ generation. This capability is ascribed to its conjugated acceptor–donor structure that reduces the energy gap between the singlet and triplet states, while its compact hyperbranched structure stiffens intramolecular motions and thus inhibits the nonradiative decay, both of which together promote the ISC process. The size distribution of **P21** was measured by dynamic light scattering and its hydrodynamic diameter ranged from 70 to 150 nm (Fig. 8C) with a zeta potential of 7.79 ± 0.75 mV. The positive charge of **P21** enables its accumulation on negatively charged bacterial membranes *via* electrostatic interactions, facilitating fluorescent labeling of MRSA within 60 min (Fig. 8D). Under dark conditions, **P21** moderately inhibited bacterial viability due to its intrinsic dark toxicity. However, upon white-light irradiation, bacterial viability was reduced by two orders of magnitude due to the synergistic effects of phototoxicity and dark toxicity. At a concentration of 30 μg mL^{-1}, **P21** achieved a bacterial killing efficiency of 99.2%, indicating its potent inactivation capability (Fig. 8E). Live/dead fluorescence staining further confirmed these effects (Fig. 8F). Under light irradiation, the bacteria displayed red fluorescence, signifying cell death, whereas under dark
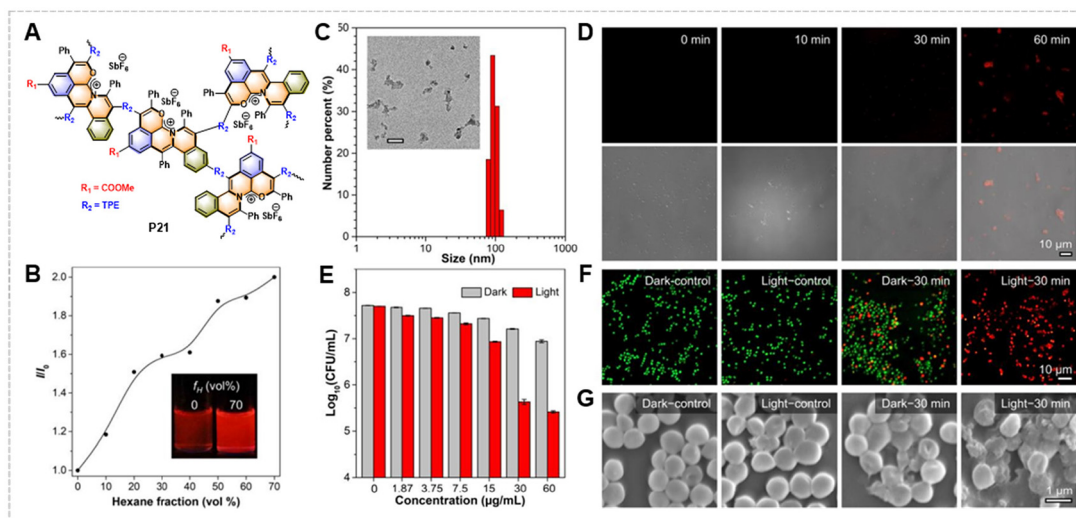
Fig. 8 (A) Structure of CMCP **P21**. (B) Plot of the relative emission intensity (I/I_0) *versus* the composition of hexane/chloroform mixtures of **P21**. Inset: photographs of **P21** in hexane/chloroform mixtures with different hexane fractions (f_H) taken under UV irradiation from a handheld UV lamp. (C) Size distribution of **P21** measured by dynamic light scattering. Inset: a TEM image of **P21** aggregates. (D) CLSM images of bacteria incubated with **P21** at different times. (E) Statistical analyses of the bacterial viability by the logarithm number in the absence and presence of white-light irradiation. (F) Live/dead staining of bacteria with different treatments. (G) SEM images of bacteria with different treatments. Adapted with permission from ref. 18. Copyright 2021 Wiley-VCH GmbH.

conditions, surviving bacteria emitted green fluorescence. Scanning electron microscopy (SEM) (Fig. 8G) revealed that, in the absence of light, bacterial membranes exhibited a rough, partially collapsed surface. Under light irradiation, the membranes showed severe splitting and deformation, likely caused by the photodynamic effect of **P21**. Apart from photodynamic antibacterial effects, some CMCPs have also been utilized in antibacterial photothermal therapy (aPTT). For instance, the previously mentioned **P19**, upon exposure to an 808 nm laser, raised the temperature of a 30 mM polymer solution to 50.68 °C within 5 minutes, effectively disrupting bacterial membrane proteins and lipids, leading to bacterial death.[31]

3.2 Fluorescence sensing

Due to their positively charged nature, polyelectrolytes selectively bind to oppositely charged analytes through electrostatic interactions. Leveraging this property, CMCPs demonstrate their applicability in fluorescence sensing.

Lu and co-workers reported preparing a novel conjugated poly(pyridinium salt) derivative (**P22**) with AIE properties *via* ring-transmutation polymerization (Fig. 9A). The CMCP aggregated with DNA through the synergistic effects of electrostatic attraction and intercalation, enabling its application in fluorescence turn-on detection. **P22** exhibited selective fluorescence enhancement upon interaction with double-stranded DNA (dsDNA), which has also been successfully used to track DNA cleavage by nuclease.[28] The cationic charge on **P22** facilitated complex formation with highly negatively charged ctDNA *via* electrostatic attraction. As shown in Fig. 9B, **P22** exhibited
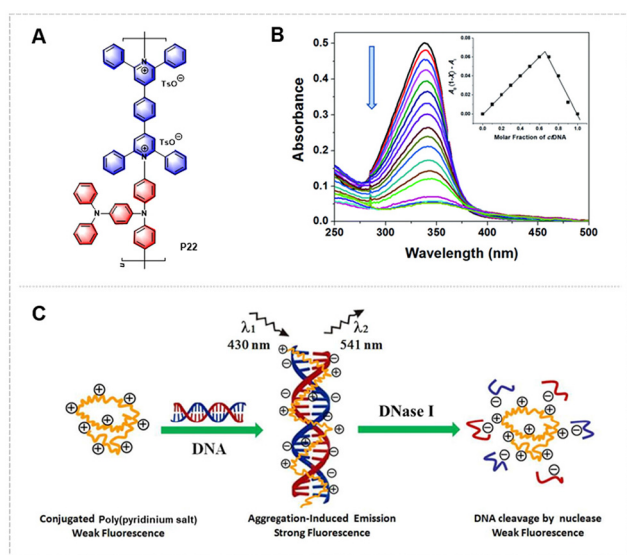

Fig. 9 (A) Structure of CMCP **P22**. (B) UV-vis absorption spectra of **P22** ([**P22**] = 5 μM) in the presence of different concentrations of ctDNA in CH_3CN-H_2O (v/v = 1 : 1). Inset: Job's plot. A_0 is the initial absorbance of free **P22**, A_i is the recorded absorbance of complexes at different ctDNA concentrations in CH_3CN-H_2O (v/v = 1 : 1), and X_i is the molar fraction of ctDNA. (C) Graphical abstract of the fluorescence sensing of DNA. Adapted with permission from ref. 28. Copyright 2015 the Royal Society of Chemistry.

a maximal absorption at 337 nm, attributed to the π–π* transition of its backbone. Upon increasing the ctDNA content, the absorbance at 337 nm decreased, accompanied by a redshift of approximately 10 nm, indicating aggregate formation between ctDNA and **P22**. Moreover, with the augmentation of the ctDNA concentration, the fluorescence intensity at 541 nm sharply increased. Compared to the weak emission of **P22** in solution, its emission intensity was enhanced 10.2 times upon the addition of ctDNA, reaching saturation at a ctDNA concentration of 23.6 μM. No obvious fluorescence increase at 541 nm was detected with various anions (including Cl^-, Br^-, HCO_3^-, HPO_4^{2-}, HSO_4^-, I^-, $P_2O_7^{4-}$, PO_4^{3-}, and SO_4^{2-}) or ssDNAs containing different base lengths, demonstrating the high selectivity of **P22** for ctDNA. This selectivity, driven by synergistic electrostatic attraction and intercalation, enhanced fluorescence emission *via* the AIE effect. When bovine pancreatic deoxyribonuclease I (DNase I), an endonuclease, was added to the mixture of ctDNA and **P22**, the fluorescence intensity gradually decreased over time (Fig. 9C). These results suggested that **P22** is a promising fluorescent probe for the development of a label-free fluorescence nuclease assay.

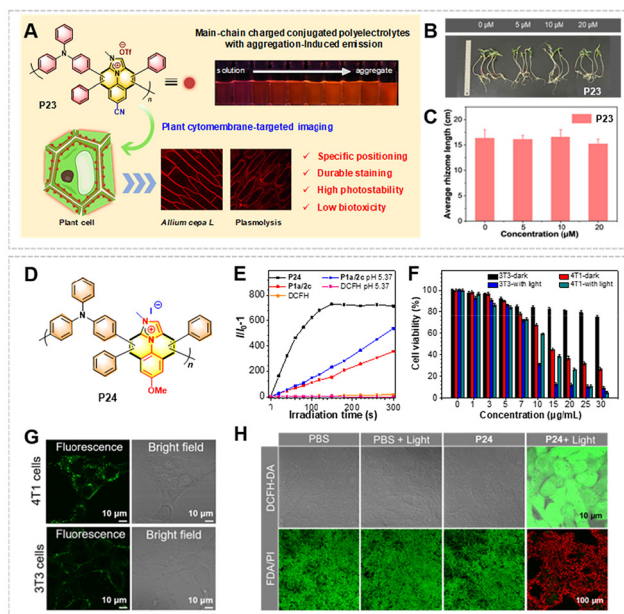### 3.3 Fluorescence imaging and cancer cell killing

Fluorescence-based imaging technologies have emerged as rapid, facile and powerful tools due to their low cost, high sensitivity, excellent signal-to-noise ratio, and remarkable reliability.[59] Numerous CMCPs have exhibited excellent fluorescence properties, with some possessing AIE features, which make them ideal for applications in fluorescence imaging of bacteria, cellular localization, and biological processes.[18,47,60]

As shown in Fig. 10A, Han *et al.* prepared a CMCP **P23** containing a TPA unit and cyano group using the CAAP strategy. **P23** was able to achieve highly specific and long-term cytomembrane imaging of plant cells.[30] Confocal laser scanning microscopy (CLSM) revealed that **P23** exhibited bright fluorescence on the onion cytomembrane, with almost no fluorescence detected in the cytoplasm and intercellular substance. Importantly, **P23** displayed long-term imaging of the plant cytomembrane, with no significant change occurring in the cytoplasm and other cellular regions for at least 12 h. The positive charge on **P23** greatly promoted its electrostatic interaction with the plant cell membrane, thereby improving its imaging capability. As shown in Fig. 10B and C, *Vigna radiata* (*V. radiata*) sprouts were obtained after treatment with **P23** at different concentrations for 7 days. The result showed that **P23** had minimal impact on the growth of *V. radiata* even at a concentration of 20 μM, implying its low biotoxicity. Besides, **P23** achieved good fluorescence imaging in other plant cells, such as *Glycine max* (*G. max*) and *V. radiata*, indicating its broad applicability. **P23** exhibited the advantages of good photostability, wash-free staining, high imaging integrity, durability and low biotoxicity, which provided a promising platform for the development of AIE-active fluorescent probes for plant plasma membranes.

In addition to fluorescence imaging, this group developed MCCP **P24** for cancer cell killing (Fig. 10D).[29] As depicted in

Fig. 10 (A) Graphical abstract of the fluorescence imaging of CMCP **P23**. (B) Photographs of representative *V. radiata* seedlings incubated with different concentrations of **P23** after 7 days. (C) Average rhizome lengths of *V. radiata* seedlings incubated without and with different concentrations of **P23** after 7 days. Adapted with permission from ref. 30. Copyright 2024 American Chemical Society. (D) Structure of CMCP **P24**. (E) ROS generation of polymers (**P24** and **P1a/P2c**, 1 μM) at pH = 5.37 and 7.40 upon white-light irradiation (24 mW cm^{-2}) using dichlorofluorescin (DCFH) as an indicator. (F) Cell viability of 3T3 and 4T1 cells incubated with **P24** without or with the irradiation of white light (24 mW cm^{-2}, 10 min). (G) CLSM images of 4T1 and 3T3 cells after incubation with **P24** (20 μg mL^{-1}) for 0.5 h. (H) CLSM imaging for intracellular ROS generation (upper row) and the live/dead cell assay (lower row) of 4T1 cells with different treatments. Adapted with permission from ref. 29. Copyright 2022 American Chemical Society.

Fig. 10E, **P24** demonstrated excellent ROS generation capability, with a 730-fold enhancement within 150 seconds. Further experiments confirmed the presence of both type I and type II ROS in **P24**. The MTT assay revealed that **P24** demonstrated a synergistic effect of dark toxicity and high phototoxicity against cancer cells (Fig. 10F). Specifically, in the dark, **P24** showed higher dark toxicity towards 4T1 cells compared to normal 3T3 cells. Upon light irradiation (24 mW cm^{-2}, 10 min), the cancer cell viability significantly decreased with the treatment of **P24**. Differences in cytotoxicity between normal and cancer cells were attributed to the varying cellular uptake levels of **P24** (Fig. 10G). As depicted in the upper row of Fig. 10H, using the ROS indicator 2′,7′-dichlorofluorescein diacetate (DCFH-DA), bright green fluorescence was observed in 4T1 cells under light irradiation, whereas no significant fluorescence appeared in the control groups. This result indicated that **P24** was able to produce ROS efficiently. The live/dead staining experiment provided visual evidence for the phototherapeutic effect of **P24** (Fig. 10H, lower row). While light-only irradiation did not cause severe cell death, red fluorescence indicative of cell death was clearly observed in **P24**-treated

cells, implying its phototoxic effect with reduced side effects. Interestingly, the authors found that green fluorescence was accompanied by faint red fluorescence in the **P24** group, which did not entirely align with the MTT assay results. They hypothesized that 4T1 cells treated with **P24** for 13 hours under dark conditions were in an early apoptotic state rather than fully dead. This hypothesis was further validated through an Annexin V-APC/PI detection assay.

3.4 Other applications

Given the effective aggregate-state fluorescence and easily adjustable electronic properties of CMCPs, their applications in the preparation of fluorescent interfacial polyelectrolyte complexation (IPC) fibers can be developed.[8]

Recently, Wang *et al.* reported a series of imidazolium-containing CMCPs (**P25–P28**) (Fig. 11A). The charge distributions of the repeating units in these CMCPs were analyzed using an electrostatic potential map (EPM), which revealed that the positively charged regions were primarily concentrated in the imidazolium moiety of the cationic ring-fused backbone
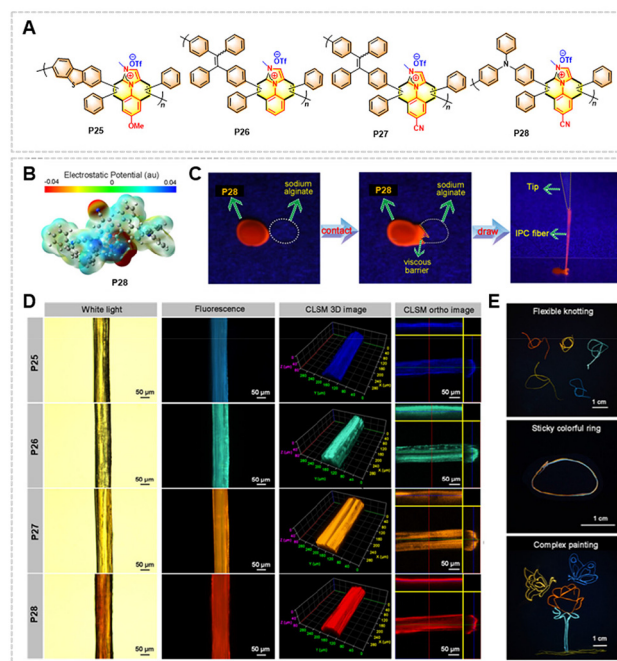
Fig. 11 (A) Structures of CMCPs (**P25–P28**). (B) Electrostatic potential surface of the repeating unit of **P28**. (C) Fluorescence photographs showing the IPC fiber drawing process under 365 nm UV irradiation. (D) Optical and fluorescence images of the freshly formed cationic CMCPs/ sodium alginate fibers captured under white light and UV light irradiation (340−380 nm), respectively, using an inverted fluorescence microscope (the front two columns of images), and their fluorescence 3D images together with the corresponding cutaway view obtained by CLSM (the latter two columns of images). (E) Diverse forms of the obtained fluorescent cationic polyelectrolyte/sodium alginate fibers. The macroscopic fluorescence images feature real colors and were directly captured using a digital camera under 365 nm UV light irradiation. Adapted with permission from ref. 8. Copyright 2023 American Chemical Society.

(Fig. 11B). This provided theoretical support for the formation of IPC fibers. As depicted in Fig. 11C, **P28** was brought into contact with sodium alginate (SA) droplets using a pipette tip, and a thin and straight IPC fiber was extracted through the interfacial interaction between polymer solutions, followed by continuous upward traction. The obtained fiber structure was fully characterized by fluorescence microscopy. As shown in Fig. 11D, most of the cationic CMCPs and anionic SA polymers were uniformly distributed in a single fiber. Fluorescence 3D images with corresponding cross-sectional views obtained through CLSM further illustrated the internal structures of fibers, where the fluorescent regions corresponded to the CMCPs, and the dark regions represented the SA components. These IPC fibers exhibited high flexibility and good adhesion, enabling the preparation of stable colorful fiber strands and fluorescent paintings (Fig. 11E). Such properties significantly broaden the application scope of CMCPs. In addition to these common applications, CMCPs also show potential in field-effect transistor devices.[48] For instance, the reported CMCP **P5** exhibited n-type behaviors with mobilities of 0.24 cm^2 $(V\ s)^{-1}$ and 3.4 cm^2 $(V\ s)^{-1}$ at gate voltages of 5–15 V and 15–20 V, respectively. Some CMCPs have also been applied in the detection of various amines. For example, Swager *et al.* reported a series of CMCPs containing various anions.[49] Among them, **P7** with perfluorinated tetraphenylborate and **P8** with tetrafluoroborate exhibited sensing abilities to simple alkyl amines and aniline, respectively. When they were exposed to the volatile amine vapors, the fluorescence of CMCPs was quenched quickly. The presence of different anions endowed polymers with the ability to differentiate amines. In the future, more CMCPs are expected to be synthesized and applied in diverse fields.

4. Conclusions

CMCPs are an important class of functional polymeric materials. In this review, we summarized the representative synthetic methods for the construction of diverse CMCPs. In addition, the applications of CMCPs in different fields, such as antimicrobial, fluorescence sensing, imaging, optoelectronic devices, *etc.*, were also introduced. Although some CMCPs have been successfully obtained by efficient synthetic strategies, there is still huge scope for the development of novel synthetic methods and applications of CMCPs. Besides, it is highly desirable to further enrich the structural and functional diversity of CMCPs. Therefore, several perspectives are discussed, which may include but are not limited to the aspects below.

First, the structure types of CMCPs are mainly limited to nitrogen-containing structures, including those based on pyridinium and imidazolium salts. Meanwhile, the charges carried by most of the available CMCPs are positive. More efforts could be devoted to introducing other ionizable heteroatoms into CMCP structures to form charged oxygen and sulfur-containing structural moieties or introducing negatively charged structural units into CMCP structures. Second, traditional methods for the synthesis of CMCPs mainly involve

ring-transmutation polymerizations, nucleophilic substitution, aldol-type condensation, *etc*. These synthetic routes are relatively complex and time-consuming. Developing facile and efficient methods is crucial for the enrichment of structural and functional diversity. Among various methods, the CAAP strategy has shown great potential in the construction of novel CMCPs with the advantages of high atom economy and step economy, a wide monomer scope, and readily functionalized fused heterocyclic units with multiple substituents, which can conveniently modulate the electronic effects of the CMCP backbones and promote the development of multifunctional fluorescent polymer materials. Furthermore, precise control over molecular weights and polydispersities is essential for the study of structure–property relationships as is fine tuning materials properties such as mechanical performance, thermal stability, and photophysical characteristics. However, it still remains challenging to synthesize CMCPs with controllable molecular weights and narrow polydispersities, which could be one of the important research directions of this field that can benefit from further improvements. The properties of CMCPs, such as optical properties, electrical conductivity, and bioactivity, can be altered easily to meet the application demands in different fields. We hope that this review will provide new inspirations and ideas for researchers to develop easier synthetic methods and construct CMCPs with more diversified structures and advanced functionalities.

Data availability

No primary research results, software or code have been included and no new data were generated or analysed as part of this review.

Conflicts of interest

There are no conflicts to declare.

Acknowledgements

References

1 V. S. Meka, M. K. G. Sing, M. R. Pichika, S. R. Nali, V. R. M. Kolapalli and P. Kesharwani, *Drug Discovery Today*, 2017, **22**, 1697–1706.

2 X. L. Liu, M. G. Li, T. Han, B. Cao, Z. Qiu, Y. Y. Li, Q. Y. Li, Y. B. Hu, Z. Y. Liu, J. W. Y. Lam, X. L. Hu and B. Z. Tang, *J. Am. Chem. Soc.*, 2019, **141**, 11259–11268.

3 T. H. Pham, J. S. Olsson and P. Jannasch, *J. Am. Chem. Soc.*, 2017, **139**, 2888–2891.

4 Y. W. Zhu, C. Xu, N. Zhang, X. K. Ding, B. R. Yu and F. J. Xu, *Adv. Funct. Mater.*, 2018, **28**, 1706709.

5 J. W. Qi, T. Y. Wu, W. K. Wang, H. J. Jin, S. T. Gao, S. S. Jiang, J. B. Huang and Y. Yan, *Aggregate*, 2022, **3**, e173.

6 S. Hussain, A. H. Malik and P. K. Iyer, *ACS Appl. Mater. Interfaces*, 2015, **7**, 3189–3198.

7 X. Q. Liu, Z. H. Shi, F. Yu, C. Teng, C. Zhang and Z. R. Chen, *Aggregate*, 2023, **4**, e363.

8 K. Wang, J. K. Liu, P. Y. Liu, D. Wang, T. Han and B. Z. Tang, *J. Am. Chem. Soc.*, 2023, **145**, 4208–4220.

9 A. Hazra and S. K. Samanta, *Langmuir*, 2024, **40**, 2417–2438.

10 J. Wang, K. Liang, J. Li, Y. X. Zhang, X. K. Xue, T. J. Chen, Y. L. Hao, J. S. Wu and J. C. Ge, *Chin. J. Polym. Sci.*, 2024, **42**, 1690–1698.

11 H. Sun, I. Barboza-Ramos, X. D. Wang and K. S. Schanze, *ACS Appl. Mater. Interfaces*, 2024, **16**, 20023–20033.

12 I. Barboza-Ramos, H. B. Gobeze, D. Wherritt and K. S. Schanze, *Macromolecules*, 2024, **57**, 7575–7585.

13 R. D. McCullough, P. C. Ewbank and R. S. Loewe, *J. Am. Chem. Soc.*, 1997, **119**, 633–634.

14 X. F. Liu, C. R. Zhang, H. W. Peng and Q. Zhao, *Chin. J. Polym. Sci.*, 2024, **42**, 984–991.

15 Y. Jin, R. Yang, H. Suh and H. Y. Woo, *Macromol. Rapid Commun.*, 2008, **29**, 1398–1402.

16 M. R. Pinto, B. M. Kristal and K. S. Schanze, *Langmuir*, 2003, **19**, 6523–6533.

17 Z. B. Henson, Y. Zhang, T. Q. Nguyen, J. H. Seo and G. C. Bazan, *J. Am. Chem. Soc.*, 2013, **135**, 4163–4166.

18 X. L. Liu, M. H. Xiao, K. Xue, M. Z. Li, D. M. Liu, Y. Wang, X. Z. Yang, Y. B. Hu, R. T. K. Kwok, A. J. Qin, C. L. Zhu, J. W. Y. Lam and B. Z. Tang, *Angew. Chem., Int. Ed.*, 2021, **60**, 19222–19231.

19 F. L. Han, Y. Lu, Q. Zhang, J. Sun, X. S. Zeng and C. X. Li, *J. Mater. Chem.*, 2012, **22**, 4106–4112.

20 J. F. Sun, Y. Lu, L. Wang, D. D. Cheng, Y. J. Sun and X. S. Zeng, *Polym. Chem.*, 2013, **4**, 4045–4051.

21 W. Gao, Z. C. Dang, F. S. Liu, S. Wang, D. W. Zhang and M. X. Yan, *RSC Adv.*, 2020, **10**, 43523–43532.

22 S. L. Kristufek, T. R. Maltais, E. G. Tennyson, N. C. Osti, D. Perahia, A. G. Tennyson and R. C. Smith, *Polym. Chem.*, 2013, **4**, 5387–5394.

23 X. Wang, G. X. Wang, J. H. Zhao, Z. Y. Zhu and J. Y. Rao, *ACS Macro Lett.*, 2021, **10**, 1643–1649.

24 A. Q. Dai, W. J. Wang, X. Y. Heng, W. J. Shu, S. P. Lu, Y. M. Xu, D. L. Wang, X. Q. Pan, N. Li, G. J. Chen and J. Zhu, *ACS Appl. Polym. Mater.*, 2024, **6**, 4975–4984.

25 N. J. Chen, H. H. Wang, S. P. Kim, H. M. Kim, W. H. Lee, C. Hu, J. Y. Bae, E. S. Sim, Y. C. Chung, J. H. Jang, S. J. Yoo, Y. B. Zhuang and Y. M. Lee, *Nat. Commun.*, 2021, **12**, 2367.

26 B. X. Xue, W. D. Cui, S. Y. Zhou, Q. F. Zhang, J. F. Zheng, S. H. Li and S. B. Zhang, *Macromolecules*, 2021, **54**, 2202–2212.

27 A. Hazra, C. Ghosh, F. Banerjee and S. K. Samanta, *ACS Appl. Polym. Mater.*, 2024, **6**, 6540–6551.

28 Y. Chang, L. Jin, J. J. Duan, Q. Zhang, J. Wang and Y. Lu, *RSC Adv.*, 2015, **5**, 103358–103364.

29 K. Wang, S. S. Yan, T. Han, Q. Wu, N. Yan, M. M. Kang, J. Y. Ge, D. Wang and B. Z. Tang, *J. Am. Chem. Soc.*, 2022, **144**, 11788–11801.

30 B. J. Huang, K. Wang, J. C. Zhang, H. W. Yan, H. Zhao, L. Han, T. Han and B. Z. Tang, *ACS Appl. Mater. Interfaces*, 2024, **16**, 20011–20022.

31 C. L. Anderson, N. Dai, S. J. Teat, B. He, S. Wang and Y. Liu, *Angew. Chem., Int. Ed.*, 2019, **58**, 17978–17985.

32 C. L. Zhu, L. B. Liu, Q. Yang, F. T. Lv and S. Wang, *Chem. Rev.*, 2012, **112**, 4687–4735.

33 R. L. Qi, H. Zhao, X. Zhou, J. Liu, N. Dai, Y. Zeng, E. D. Zhang, F. T. Lv, Y. M. Huang, L. B. Liu, Y. L. Wang and S. Wang, *Angew. Chem., Int. Ed.*, 2021, **60**, 5759–5765.

34 A. Parthasarathy, H. C. Pappas, E. H. Hill, Y. Huang, D. G. Whitten and K. S. Schanze, *ACS Appl. Mater. Interfaces*, 2015, **7**, 28027–28034.

35 C. L. Zhu, Q. Yang, L. B. Liu and S. Wang, *Chem. Commun.*, 2011, **47**, 5524–5526.

36 D. Aili, J. Yang, K. Jankova, D. Henkensmeier and Q. F. Li, *J. Mater. Chem. A*, 2020, **8**, 12854–12886.

37 Z. Chen, H. X. Yuan and H. Y. Liang, *ACS Appl. Mater. Interfaces*, 2017, **9**, 9260–9264.

38 L. J. Mei, C. Li, P. J. Zhao, T. Chen, R. Tian, J. Guo and M. Q. Zhu, *Macromol. Rapid Commun.*, 2022, **43**, 2100899.

39 S. L. Suraru, J. A. Lee and C. K. Luscombe, *ACS Macro Lett.*, 2016, **5**, 724–729.

40 B. Wang, B. N. Queenan, S. Wang, K. P. R. Nilsson and G. C. Bazan, *Adv. Mater.*, 2019, **31**, 1806701.

41 H. Jiang, P. Taranekar, J. R. Reynolds and K. S. Schanze, *Angew. Chem., Int. Ed.*, 2009, **48**, 4300–4316.

42 Y. Liu, V. V. Duzhko, Z. A. Page, T. Emrick and T. P. Russell, *Acc. Chem. Res.*, 2016, **49**, 2478–2488.

43 P. K. Bhowmik, H. Han and A. K. Nedeltchev, *Polymer*, 2006, **47**, 8281–8288.

44 P. K. Bhowmik, T. S. Jo, J. J. Koh, J. Park, B. Biswas, R. C. G. Principe, H. Han, A. E. Wacha and M. Knaapila, *Molecules*, 2021, **26**, 1560.

45 T. T. Do, H. S. Hong, Y. E. Ha, J. Park, Y. C. Kang and J. H. Kim, *ACS Appl. Mater. Interfaces*, 2015, **7**, 3335–3341.

46 T. S. Lee, H. Ahn, W. H. Park, B. H. Sohn, M. J. Kim and D. Y. Kim, *J. Polym. Sci., Part A: Polym. Chem.*, 2003, **41**, 1196–1201.

47 Z. G. He, X. J. Han, Z. F. Yan, B. Guo, Q. Cai and Y. W. Yao, *Mater. Chem. Front.*, 2022, **6**, 3678–3690.

48 D. Izuhara and T. M. Swager, *J. Am. Chem. Soc.*, 2009, **131**, 17724–17725.

49 S. Rochat and T. M. Swager, *Angew. Chem., Int. Ed.*, 2014, **53**, 9792–9796.

50 A. Merz and D. C. S. Reitmeier, *Angew. Chem., Int. Ed. Engl.*, 1989, **28**, 807–808.

51 C. Y. Li, W. H. Liu, B. N. Wang, A. J. Qin and B. Z. Tang, *ChemRxiv*, 2024, preprint, DOI: **10.26434/chemrxiv-2024-r1vxg.**

52 D. Y. Fan, D. L. Wang, J. Zhang, X. Y. Fu, X. K. Yan, D. Wang, A. J. Qin, T. Han and B. Z. Tang, *J. Am. Chem. Soc.*, 2024, **146**, 17270–17284.

53 Y. Zhang, L. Zhao, P. K. Patra, D. Y. Hu and J. Y. Ying, *Nano Today*, 2009, **4**, 13–20.

54 J. N. Guo, J. Qin, Y. Y. Ren, B. Wang, H. Q. Cui, Y. Y. Ding, H. L. Mao and F. Yan, *Polym. Chem.*, 2018, **9**, 4611–4616.

55 J. T. Fan, A. G. Wright, B. Britton, T. Weissbach, T. J. G. Skalski, J. Ward, T. J. Peckham and S. Holdcroft, *ACS Macro Lett.*, 2017, **6**, 1089–1093.

56 J. T. Fan, S. Willdorf-Cohen, E. M. Schibli, Z. Paula, W. Li, T. J. G. Skalski, A. T. Sergeenko, A. Hohenadel, B. J. Frisken, E. Magliocca, W. E. Mustain, C. E. Diesendruck, D. R. Dekel and S. Holdcroft, *Nat. Commun.*, 2019, **10**, 2306.

57 Q. S. Zhang, Master thesis, South China University of Technology, 2019.

58 S. W. Guo, Q. X. Huang, Y. Chen, J. W. Wei, J. Zheng, L. Y. Wang, Y. T. Wang and R. B. Wang, *Angew. Chem., Int. Ed.*, 2021, **60**, 618–623.

59 M. M. Kang, C. C. Zhou, S. M. Wu, B. R. Yu, Z. J. Zhang, N. Song, M. M. S. Lee, W. H. Xu, F. J. Xu, D. Wang, L. Wang and B. Z. Tang, *J. Am. Chem. Soc.*, 2019, **141**, 16781–16789.

60 R. Chen, X. Y. Gao, X. Cheng, A. J. Qin, J. Z. Sun and B. Z. Tang, *Polym. Chem.*, 2017, **8**, 6277–6282.